Stereochemical Control of Hairpin Formation in β-Peptides Containing Dinipecotic Acid Reverse Turn Segments

Yong Jun Chung, Bayard R. Huck, Laurie A. Christianson, Heather E. Stanger, Susanne Krauthäuser, Douglas R. Powell, and Samuel H. Gellman*

Contribution from the Department of Chemistry, University of Wisconsin, Madison, Wisconsin 53706

Received September 20, 1999. Revised Manuscript Received February 23, 2000

Abstract: We examine the relationship between covalent structure and conformational propensity among a series of β-amino acid tetramers. These experiments focus on the hairpin folding motif. Among conventional peptides, the minimum increment of β-sheet secondary structure is a "β-hairpin," in which two strands are connected via a short loop. The present studies are aimed at optimizing hairpin stability among β-peptides. Previous work from our laboratory has identified optimal substitution patterns for residues that form strands in an antiparallel β-peptide sheet (Krauthäuser et al. *J. Am. Chem. Soc.* **1997**, *119*, 11719), and we have shown that a dinipecotic acid segment can promote sheet-type interactions between attached strand residues (Chung et al. *J. Am. Chem. Soc.* **1998**, *120*, 10555). Here we compare all four possible configurations of the dinipecotic acid segment, (*R*,*S*), (*S*,*R*), (*R*,*R*) and (*S*,*S*), for the ability to induce sheet formation with a constant set of enantiomerically pure strand residues. We show that both heterochiral dinipecotic acid segments promote hairpin formation, although one is distinctly superior. Neither of the homochiral dinipecotic acid supports hairpin folding. When the strand residues are β-alanine (achiral), the heterochiral dinipecotic acid segment is again superior to the homochiral segment, but we find a difference between hairpin conformations in solution and in the solid state.

Introduction

Unnatural oligomers with well-defined folding behavior ("foldamers") are subjects of increasing interest.[1] Biological systems rely almost exclusively on well-folded polymers (proteins and RNA) for complex molecular functions such as catalysis, and it might be possible to engineer comparable functions into unnatural foldamers. Numerous recent reports have described oligomers that adopt specific secondary structures,[2−21] especially helices; collectively these efforts represent important progress toward a long-range goal of creating unnatural tertiary structures.

(1) Recent reviews: (a) Gellman, S. H. *Acc. Chem. Res.* **1998**, *31*, 173. (b) Kirshenbaum, K.; Zuckermann, R. N.; Dill, K. A. *Curr. Opin. Struct. Biol.* **1999**, *9*, 530. (c) Stigers, K. D.; Soth, M. J.; Nowick, J. S. *Curr. Opin. Chem. Biol.* **1999**, *3*, 714. (d) Barron, A. E.; Zuckermann, R. N. *Curr. Opin. Chem. Biol.* **1999**, *3*, 681.

(2) Helical β-peptide oligomers: (a) Seebach, D.; Overhand, M.; Kühnle, F. N. M.; Martinoni, B.; Oberer, L.; Hommel, U.; Widmer, H. *Helv. Chim. Acta* **1996**, *79*, 913. (b) Seebach, D.; Ciceri, P.; Overhand, M.; Juan, B.; Rigo, D.; Oberer, L.; Hommel, U.; Amstutz, R.; Widmer, H. *Helv. Chim. Acta* **1996**, *79*, 2043. (c) Seebach, D.; Matthews, J. L. *J. Chem. Soc., Chem. Commun.* **1997**, 2015−2022. (d) Seebach, D.; Abele, S.; Gademann, K.; Guichard, G.; Hintermann, T.; Jaun, B.; Matthews, J. L.; Schreiber, J.; Oberer, L.; Hommel, U.; Widmer, H. *Helv. Chim. Acta* **1998**, *81*, 932. (e) Seebach, D.; Abele, S.; Sifferlen, T.; Hänggi, M.; Gruner, S.; Seiler, P. *Helv. Chim. Acta* **1998**, *81*, 2218.

(3) Helical β-peptide oligomers: (a) Appella, D. H.; Christianson, L. A.; Karle, I. L.; Powell, D. R.; Gellman, S. H. *J. Am. Chem. Soc.* **1996**, *118*, 13071. (b) Appella, D. H.; Christianson, L. A.; Klein, D. A.; Powell, D. R.; Huang, X.; Barchi, J. J.; Gellman, S. H. *Nature* **1997**, *387*, 381. (c) Applequist, J.; Bode, K. A.; Appella, D. H.; Christianson, L. A.; Gellman, S. H. *J. Am. Chem. Soc.* **1998**, *120*, 4891. (d) Appella, D. H.; Barchi, J. J.; Durell, S.; Gellman, S. H. *J. Am. Chem. Soc.* **1999**, *121*, 2309. (e) Appella, D. H.; Christianson, L. A.; Karle, I. L.; Powell, D. R.; Gellman, S. H. *J. Am. Chem. Soc.* **1999**, *121*, 6206. (f) Appella, D. H.; Christianson, L. A.; Klein, D. A.; Richards, M. R.; Powell, D. R.; Gellman, S. H. *J. Am. Chem. Soc.* **1999**, *121*, 7574. (g) Wang, X.; Espinosa, J. F.; Gellman, S. H., *J. Am. Chem. Soc.*, in press.

(4) Gung, B. W.; Zou, D.; Stalcup, A. M.; Cottrell, C. E. *J. Org. Chem.* **1999**, *64*, 2176.

(5) Computer simulations of β-peptides: (a) Daura, X.; van Gunsteren, W. F.; Rigo, D.; Jaun, B.; Seebach, D. *Chem. Eur. J.* **1997**, *3*, 1410. (b) Christianson, L. A., Ph.D. Thesis, University of Wisconsin-Madison, 1997. (c) Daura, X.; Jaun, B.; Seebach, D.; van Gunsteren, W. F.; Mark, A. *J. Mol. Biol.* **1998**, *280*, 925. (d) Daura, X.; Gademann, K.; Jaun, B.; Seebach, D.; van Gunsteren, W. F.; Mark, A. E. *Angew. Chem., Int. Ed.* **1999**, *38*, 236. (e) Daura, X.; van Gunsteren, W. F.; Mark, A. E. *Proteins: Struct., Funct., Genet.* **1999**, *34*, 269. (f) Wu, Y. D.; Wang, D. P. *J. Am. Chem. Soc.* **1998**, *120*, 13485. (g) Möhle, K.; Günther, R.; Thormann, N.; Hofmann, H.-J. *Biopolymers* **1999**, *50*, 167.

(6) Hairpin-forming β-peptides: (a) Krauthäuser, S.; Christianson, L. A.; Powell, D. R.; Gellman, S. H. *J. Am. Chem. Soc.* **1997**, *119*, 11719. (b) Chung, Y. J.; Christianson, L. A.; Stanger, H. E.; Powell, D. R.; Gellman, S. H. *J. Am. Chem. Soc.* **1998**, *120*, 10555. (c) Seebach, D.; Abele, S.; Gademann, K.; Jaun, B. *Angew. Chem., Int. Ed.* **1999**, *38*, 1595.

(7) β-Peptide nucleic acid analogues: Diederichsen, U.; Schmitt, H. W. *Eur. J. Org. Chem.* **1998**, 827.

(8) Vinylogous peptide folding: Hagihara, M.; Anthony, N. J.; Stout, T. J.; Clardy, J.; Schreiber, S. L. *J. Am. Chem. Soc.* **1992**, *114*, 6568.

(9) Nucleic acid analogue folding: Beier, M.; Reck, F.; Wagner, T.; Krishnamurthy, R.; Eschenmoser, A. *Science* **1999**, *283*, 699 and references therein.

(10) Aedamer folding: (a) Lokey, R. S.; Iverson, B. L. *Nature* **1995**, *375*, 303. (b) Nguyen, J. Q.; Iverson, B. L. *J. Am. Chem. Soc.* **1999**, *121*, 2639.

(11) Sulfonamide oligomer folding: Gennari, C.; Salom, B.; Potenza, D.; Longari, C.; Fioravanzo, E.; Carugo, O.; Sardone, N. *Chem. Eur. J.* **1996**, *2*, 644 and references therein.

(12) γ-Peptide folding: (a) Hintermann, T.; Gademann, K.; Jaun, B.; Seebach, D. *Helv. Chim. Acta* **1998**, *81*, 983. (b) Hanessian, S.; Luo, X.; Schaum, R.; Michnick, S. *J. Am. Chem. Soc.* **1998**, *120*, 8569. (c) Hanessian, S.; Luo, X.; Schaum, R. *Tetrahedron Lett.* **1999**, *40*, 4925.

(13) δ-Peptide folding: (a) Szabo, L.; Smith, B. L.; McReynolds, K. D.; Parrill, A. L.; Morris, E. R.; Gervay, J. *J. Org. Chem.* **1998**, *63*, 1074. (b) Smith, M. D.; Claridge, T. D. W.; Tranter, G. E.; Sansom, M. S. P.; Fleet, G. W. J. *J. Chem. Soc., Chem. Commun.* **1998**, 2041. (c) Long, D. D.; Hungerford, N. L.; Smith, M. D.; Brittain, D. E. A.; Marquess, D. G.; Claridge, T. D. W.; Fleet, G. W. J. *Tetrahedron Lett.* **1999**, *40*, 2195. (d) Claridge, T. D. W.; Long, D. D.; Hungerford, N. L.; Aplin, R. T.; Smith, M. D.; Marquess, D. G.; Fleet, G. W. J. *Tetrahedron Lett.* **1999**, *40*, 2199.

10.1021/ja993416p CCC: $19.00
Published on Web 04/12/2000

Oligomers of β-amino acids ("β-peptides") are among the most thoroughly studied unnatural foldamers at present.[2−7] Early work on β-amino acid homopolymers suggested that both sheet[22] and helix[23] secondary structures are accessible. Helix formation by short β-peptide oligomers in organic solvents has been demonstrated via NMR by Seebach et al.[2] and by us[3]; we have been able to correlate solution data with crystal structures.[3] Recently, we have shown that β-peptide hexamers can adopt stable helical conformations in aqueous solution if the residues are properly selected.[24]

It is more difficult to generate small increments of sheet than small increments of helix because helices form along a covalently continuous segment, while sheets form from strand segments that can be widely separated along the polymer backbone.[25] To create a unimolecular sheet, one must identify residues that have a high propensity to form strands and residues that have a high propensity to form a reverse turn or loop that will induce sheet interactions between attached strand segments. Among conventional peptides and proteins, the strand−loop−strand motif is designated a "β-hairpin",[26] and we retain the term "hairpin" in our discussion of β-peptides. A hairpin represents the smallest increment of autonomously folding sheet secondary structure. Considerable effort has been devoted to the development of conventional peptides[26] (α-amino acid residues) and peptidomimetics[27] that display hairpin conformations. Hairpin-forming peptides have proven to be a good source of catalysts for stereoselective chemical transformations.[28]

We have identified an optimal β-amino acid substitution pattern for the strand residues in an antiparallel sheet through the use of hairpin-forming molecules that contain non-β-peptide loop segments.[6a] α,β-Disubstituted residues, with the appropriate configurations at the α- and β-carbons, are expected to favor an anti torsion angle about the $NC_\beta-C_\alpha C(=O)$ bond, and we showed that such residues are predisposed to form a β-peptide sheet.[6a] We have subsequently focused on replacing the non-β-peptide loop in our initial hairpins[6a] with a β-peptide loop.[6b] In a preliminary report, we described a loop segment containing two nipecotic acid residues that adopts a reverse turn conformation and promotes hairpin formation.[6b] (This β-peptide reverse turn is reminiscent of the common β-turn in conventional peptides and proteins.[29]) The resulting tetra-β-peptide represents the first autonomously folding β-peptide sheet. This accomplishment completed the demonstration that each of the three types of regular secondary structure observed in proteins, helix, sheet, and reverse turn can also be formed by β-peptides.

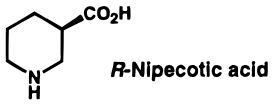

R-Nipecotic acid

Here, we present a systematic evaluation of dinipecotic acid turn segment configuration with regard to hairpin formation. We have examined two types of strand residue, enantiomerically pure α,β-disubstituted residues, and β-alanine, because prior results indicate that each strand type favors a distinct form of β-peptide sheet.[6a] We also use the current body of literature on β-peptide hairpins,[6] which includes a β-peptide hairpin very recently reported by Seebach et al.,[6c] to formulate general rules for design and analysis of autonomously folding β-peptide sheets.

Results

Synthesis. The tetra-β-peptides discussed below were prepared in solution via standard coupling reactions, which involved 1-[3-(dimethylamino)propyl]-3-ethylcarbodiimide hydrochloride (EDC) and 1-hydroxybenzotriazole (HOBt) in dimethylformamide (DMF). The Boc group was used for amino protection. We prepared the optically active α-methyl-β-ethyl strand residue by following the route of Jefford and McNulty;[30] straighforward extrapolation from this route provided the α-benzyl-β-(thiophenyl)methyl derivative.[6a] (Complete experimental details for these two α,β-disubstituted residues are provided in the Supporting Information for ref 6a.) Racemic nipecotic acid is commerically available. Resolution of enantiomers can be achieved by cocrystallization of racemic ethyl nipecotate (Nip-OC_2H_5) with enantiomerically pure tartaric acid, and repeated recrystallization of the resulting salt.[31,32] We devised an alternative resolution in which racemic nipecotic acid itself is cocrys-

(14) Oligourea folding: Nowick, J. S.; Mahrus, S.; Smith, E. M.; Ziller, J. W. *J. Am. Chem. Soc.* **1996**, *118*, 1066.

(15) Anthranilic acid oligomer folding: Hamuro, Y.; Geib, S. J.; Hamilton, A. D. *J. Am. Chem. Soc.* **1997**, *119*, 10587 and references therein.

(16) Peptoid folding: (a) Armand, P.; Kirshenbaum, K.; Goldsmith, R. A.; Farr-Jones, S.; Barron, A. E.; Truong, K. T.; Dill, K. A.; Mierke, D. F.; Cohen, F. E.; Zuckermann, R. N.; Bradley, E. K. *Proc. Natl. Acad. Sci. U.S.A.* **1998**, *95*, 4309. (b) Kirshenbaum, K.; Barron, A. E.; Goldsmith, R. A.; Armand, P.; Bradley, E. K.; Truong, K. T.; Dill, K. A.; Cohen, F. E.; Zuckermann, R. N. *Proc. Natl. Acad. Sci. U.S.A.* **1998**, *95*, 4303.

(17) *m*-Phenylacetylene oligomer folding: (a) Nelson, J. C.; Saven, J. G.; Moore, J. S.; Wolynes, P. G. *Science* **1997**, *277*, 1793. (b) Prince, R. B.; Okada, T.; Moore, J. S. *Angew. Chem., Int. Ed.* **1999**, *38*, 233. (c) Gin, M. S.; Yokozawa, T.; Prince, R. B.; Moore, J. S. *J. Am. Chem. Soc.* **1999**, *121*, 2643.

(18) α-Aminooxy acid oligomer folding: Yang, D.; Qu, J.; Li, B.; Ng, F.; Wang, X.; Cheung, K.; Wang, D.; Wu, Y. *J. Am. Chem. Soc.* **1999**, *121*, 589 and references therein.

(19) Guanidine oligomer folding: Tanatani, A.; Yamaguchi, K.; Azumaya, I.; Fukutomi, R.; Shudo, K.; Kagechika, H. *J. Am. Chem. Soc.* **1998**, *120*, 6433 and references therein.

(20) Oligopyrrolinone conformations: Smith, A. B.; Guzman, M. C.; Sprengler, P. A.; Keenan, T. P.; Holcomb, R. C.; Wood, J. L.; Carroll, P. J.; Hirschmann, R. *J. Am. Chem. Soc.* **1994**, *116*, 9947.

(21) Pyridine/pyrimidine oligomer folding: (a) Bassani, D. M.; Lehn, J.-M.; Baum, G.; Fenske, D. *Angew. Chem., Int. Ed. Engl.* **1997**, *36*, 1845. (b) Bassani, D. M.; Lehn, J.-M. *Bull. Soc. Chim. Fr.* **1997**, *134*, 897.

(22) (a) Bestian, H. *Angew. Chem., Int. Ed. Engl.* **1968**, *7*, 278. (b) Glickson, J. D.; Applequist, J. *J. Am. Chem. Soc.* **1971**, *93*, 3276. (c) Narita, M.; Doi, M.; Kudo, K.; Terauchi, Y. *Bull. Chem. Soc. Jpn.* **1986**, *59*, 3553. (d) Kovacs, J.; Ballina, R.; Rodin, R. L.; Balasubramanian, D.; Applequist, J. *J. Am. Chem. Soc.* **1965**, *87*, 119. (e) Chen, F.; Lepore, G.; Goodman, M. *Macromolecules* **1974**, *7*, 779. (f) Yuki, H.; Okamoto, Y.; Taketani, Y.; Tsubota, T.; Marubayashi, Y. *J. Polym. Sci. Polym. Chem. Ed.* **1978**, *16*, 2237.

(23) (a) Fernández-Santin, J. M.; Aymamí, J.; Rodríguez-Galán, A.; Muñoz-Guerra, S.; Subirana, J. A. *Nature* **1984**, *311*, 53. (b) Fernández-Santin, J. M.; Muñoz-Guerra, S.; Rodríguez-Galán, A.; Aymamí, J.; Lloveras, J.; Subirana, J. A.; Giralt, E.; Ptak, M. *Macromolecules* **1987**, *20*, 62. (c) Bella, J.; Alemán, C.; Fernández-Santin, J. M.; Alegre, C.; Subirana, J. A. *Macromolecules* **1992**, *25*, 5225. (d) López-Carrasquero, F.; Alemán, C.; Muñoz-Guerra, S. *Biopolymers* **1995**, *36*, 263. (e) Bode, K. A.; Applequist, J. *Macromolecules* **1997**, *30*, 2144.

(24) High-resolution structural characterization of β-peptide folding in water is described in refs 3d and 3 g. For other studies in aqueous solution, see refs 2e and 4.

(25) Nesloney, C. L.; Kelly, J. W. *Bioorg. Med. Chem.* **1996**, *4*, 739.

(26) (a) Gellman, S. H. *Curr. Opin. Chem. Biol.* **1998**, *2*, 717. (b) Lacroix, E.; Kortemme, T.; de la Paz, M. L.; Serrano, L. *Curr. Opin. Struct. Biol.* **1999**, *9*, 487.

(27) (a) Nowick, J. S. *Acc. Chem. Res.* **1999**, *32*, 287. (b) Hanessian, S.; McNaughton-Smith, G.; Lombart, H.-G.; Lubell, W. D. *Tetrahedron* **1997**, *53*, 12789. (c) Belvisi, L.; Gennari, C.; Mielgo, A.; Potenza, D.; Scolastico, C. *Eur. J. Org. Chem.* **1999**, 389. (d) Halab, L.; Lubell, W. D. *J. Org. Chem.* **1999**, *64*, 3312.

(28) (a) Gilbertson, S. R.; Pawlick, R. V. *Angew. Chem., Int. Ed. Engl.* **1996**, *35*, 902. (b) Jarvo, E. R.; Copeland, G. T.; Papaioannou, N.; Bonitatebus, P. J.; Miller, S. J. *J. Am. Chem. Soc.* **1999**, *121*, 11638.

(29) Rose, G. D.; Gierasch, L. M.; Smith, J. A. *Adv. Protein Chem.* **1985**, *37*, 1.

(30) Jefford, C. W.; McNulty, J. *Helv. Chim. Acta* **1994**, *77*, 2142.

(31) Akkerman, A. M.; de Jongh, D. K.; Veldstra, H. *Recl. Trav. Chim. Pay-Bas* **1951**, *70*, 899.

(32) Magnus, P.; Thurston, L. S. *J. Org. Chem.* **1991**, *56*, 1166.

tallized with enantiomerically pure camphorsulfonic acid. Enantiomeric purity was determined via HPLC (Chiracel OD column) after the nipecotic acid had been Boc-protected on the nitrogen and converted to the 2-naphthylmethyl ester. HPLC analysis indicated that both resolution methods provide each enantiomer of nipecotic acid in ≥98% e.e.

Conformational Analysis of Tetra-*β*-peptides Containing α,*β*-Disubstituted Strand Residues. Diastereomeric *β*-peptides **1**−**4** were examined to elucidate the effect of loop segment configuration on hairpin conformational stability. In this series, all four configurations of the dinipecotic acid reverse turn segment [(*R*,*S*), (*S*,*R*), (*R*,*R*), and (*S*,*S*)] are evaluated while the strand residues are kept constant. The comparison was carried out in a relatively nonpolar solvent, methylene chloride. Under these conditions, intramolecular hydrogen bonding provides a modest but not overwhelming driving force for adoption of compact conformations, as we have previously shown in our study of *β*-hairpin formation by conventional tetrapeptides.[33] Thus, comparing the folding of **1**−**4** in methylene chloride allows us to determine whether the turn-forming propensity of each dinipecotic acid segment is compatible with sheet-type interactions between the attached α,*β*-disubstituted residues.

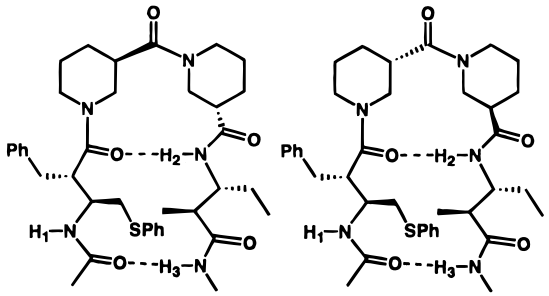

1 **2**

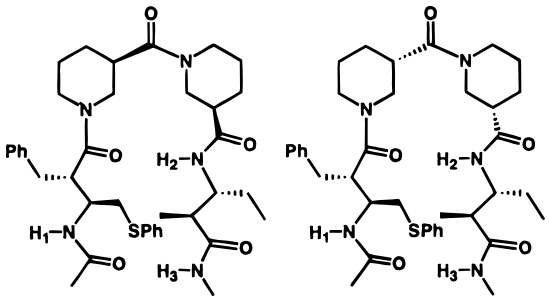

3 **4**

Two-dimensional NMR data for **1** demonstrate that a hairpin conformation is highly populated in CD_2Cl_2 (these data are available in graphical summary form in ref 6b, and in complete detail in the Supporting Information for ref 6b). Numerous NOEs are observed between the two strand residues. NOEs between adjacent residues show that the tertiary amide group linking the first and second residues has a Z configuration and the tertiary amide group linking the two nipecotic acid residues has an E configuration. The crystal structure of tetra-*β*-peptide **5**, a synthetic precursor of **1** containing a Boc group at the N-terminus, shows that the same hairpin conformation forms in the solid state.[6b] The high-resolution structural evidence for hairpin formation by **1** and close analogue **5** is complemented

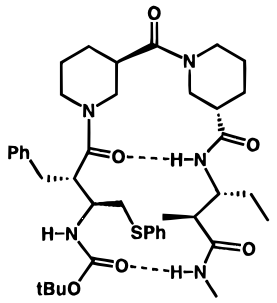

5

here by three other measurements: amide proton NMR chemical shifts, N−H stretch region IR spectra, and tertiary amide rotamer ratios detected by NMR. These three measurements provide a basis for comparing the folding behavior of diastereomers **1**−**4** in solution.

Amide proton chemical shifts (*δ*NH) are very sensitive indicators of hydrogen bond formation in nonpolar solvents such as methylene chloride.[33,34] Amide protons engaged in N−H- -O═C hydrogen bonds are typically shifted downfield by ∼2 ppm relative to non-hydrogen bonded amide protons. If the NMR measurements are carried out at sufficient dilution to preclude intermolecular interactions, then hydrogen bonding detected in this way is strictly intramolecular. Figure 1 shows the concentration dependence of *δ*NH for the three amide protons of **1** in CD_2Cl_2. There is little variation between 0.01 mM and 1.0 mM, which suggests that there is no intermolecular hydrogen bonding at or below 1 mM. The slight upward curvature observed for NH1 above 1 mM suggests that some hydrogen bond-mediated self-association occurs in this concentration range. Equilibration between non-hydrogen bonded and hydrogen bonded forms is usually rapid on the NMR time scale for small oligoamides such as those discussed here; therefore, observed *δ*NH values are population-weighted averages of the contributing hydrogen bonded and non-hydrogen bonded forms.

N−H stretch region IR data also provide insight on hydrogen bond formation in nonpolar solvents.[33,34] Non-hydrogen bonded secondary amide N−H stretch bands typically appear between 3400 and 3500 cm^{-1}, while formation of N−H- -O═C hydrogen bonds leads to N−H stretch bands between 3250 and 3400 cm^{-1}. The time scale of the IR measurement is short enough that hydrogen bonded and non-hydrogen bonded states give rise to distinct signals, in contrast to NMR measurements. IR spectroscopy has a disadvantage relative to NMR spectroscopy, however, in that N−H signals from different secondary amides within a molecule tend to overlap in the IR but not the NMR spectrum

Interconversion between tertiary amide rotamers is generally slow enough that each rotamer will give rise to a distinct set of signals in the NMR spectrum at room temperature.[35] This interconversion is fast enough, however, for equilibrium to be reached rapidly at room temperature. Determination of rotamer proportions among **1**−**4** provides indirect information on the

(33) (a) Haque, T. S.; Little, J. C.; Gellman, S. H. *J. Am. Chem. Soc.* **1994**, *116*, 4105. (b) Haque, T. S.; Little, J. C.; Gellman, S. H. *J. Am. Chem. Soc.* **1996**, *118*, 6975. (c) Stanger, H. L.; Gellman, S. H. *J. Am. Chem. Soc.* **1998**, *120*, 4236. (d) For related work, see: Raghothama, S. R.; Awasthi, S. K.; Balaram, P. *J. Chem. Soc., Perkin Trans. 2* **1998**, 137.

(34) Leading references on the use of NMR and IR data to determine internal hydrogen bonding patterns of oligoamides in nonpolar solvents: (a) Gellman, S. H.; Dado, G. P.; Liang, G.-B.; Adams, B. R. *J. Am. Chem. Soc.* **1991**, *113*, 1164. (b) Dado, G. P.; Gellman, S. H. *J. Am. Chem. Soc.* **1994**, *116*, 1054. (c) Tsang, K. Y.; Diaz, H.; Graciani, N.; Kelly, J. W. *J. Am. Chem. Soc.* **1994**, *116*, 3988. (d) Nowick, J. S.; Abdi, M.; Bellamo, K. A.; Love, J. A.; Martinez, E. J.; Noronha, G.; Smith, E. M.; Ziller, J. W. *J. Am. Chem. Soc.* **1995**, *117*, 89. (e) Gung, B. W.; Zhu, Z. *J. Org. Chem.* **1996**, *61*, 6482. (f) Yang, J.; Christianson, L. A.; Gellman, S. H. *Org. Lett.* **1999**, *1*, 11.

(35) Stewart, W. E.; Siddall, T. H. *Chem. Rev.* **1970**, *70*, 517.

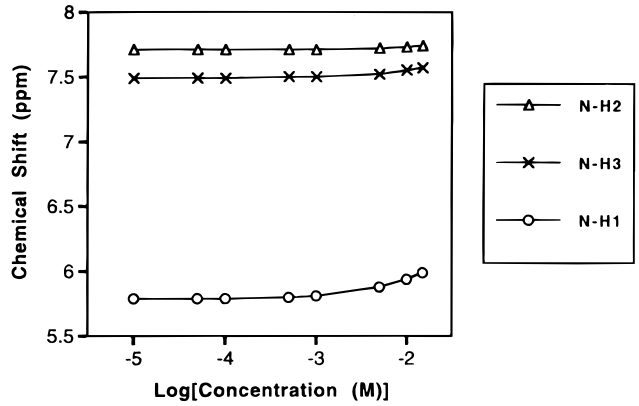

Figure 1. Amide proton NMR chemical shifts of **1** in CD_2Cl_2 at room temp, as a function of the logarithm of β-peptide concentration: (○), NH-1; (△), NH-2; (×), NH-3.

Table 1. NMR Data for Diastereomeric Tetra-β-peptides

diastereomer	% major rotamer	δNH1[a]	δNH2[a]	δNH3[a]
1	94[b]	5.80	7.71	7.49
2	78[b]	5.81	7.32	7.41
3	82[c]	5.90	6.14	6.15
4	67[c]	5.73	6.46	5.88

[a] δNH values for major rotamer. [b] One minor rotamer. [c] Two minor rotamers.

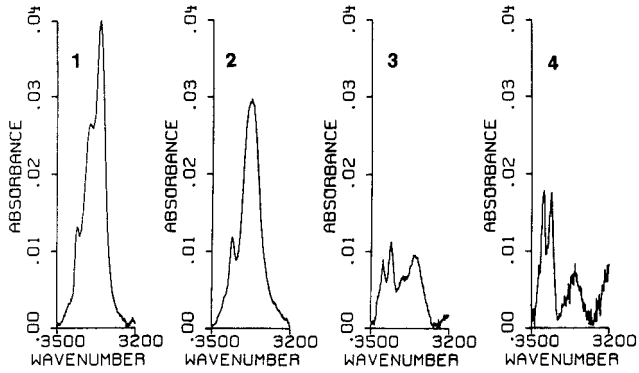

Figure 2. N−H stretch FT-IR data for 1 mM samples in CH_2Cl_2 at room temp, after subtraction of the spectrum of pure CH_2Cl_2. From left to right: **1**, maxima at 3421, 3373, and 3333 cm^{-1}; **2**, maxima at 3425 and 3354 cm^{-1}; **3**, maxima at 3454, 3425, 3378 (shoulder), and 3337 cm^{-1}; **4**, maxima at 3455, 3425, and 3338 cm^{-1}.

folding of these molecules because the hairpin conformation observed for **1** requires the nitrogens of the first and second nipecotic acid residues to be involved in tertiary amide bonds with Z and E configurations, respectively (numbering from N-to-C, as with conventional peptides).

Table 1 provides δNH values for diastereomers **1**−**4** and indicates the population of the major rotamer in CD_2Cl_2. N−H stretch region IR data for diastereomeric tetra-β-peptides **1**−**4** are shown in Figure 2.

The data for **1** are consistent with the hairpin conformation revealed by two-dimensional NMR analysis.[6b] A single rotameric form of **1** predominates in CD_2Cl_2,[36] and the amide proton chemical shift pattern reflects the expected intramolecular hydrogen bonding pattern. Thus, both δNH2 (7.71) and δNH3 (7.49) occur in a range that suggests extensive intramolecular hydrogen bond formation, while δNH1 (5.80) indicates little hydrogen bonding. The hydrogen bonding at NH2 ("inner") involves the 12-membered N−H- -O=C interaction that is associated with reverse turn formation across the dinipecotic acid reverse turn segment. The hydrogen bonding at NH3 ("outer") involves the 20-membered ring N−H- -O=C interaction that defines the hairpin conformation. The IR data for **1** show that most absorbance in the N−H stretch region occurs in the hydrogen bonded region. The small band in the non-hydrogen bonded region (3421 cm^{-1}) must arise largely from NH1, which does not form an intramolecular hydrogen bond in the hairpin conformation, as established by two-dimensional NMR and crystallographic data.[6b]

The data for **2**, which contains the alternative heterochiral turn segment, are similar to the data for **1**; therefore, the (*S*,*R*) dinipecotic acid unit of **2** also promotes hairpin formation. The principal difference between **2** and **1** is the larger population of a minor rotamer in **2**, which suggests that the (*S*,*R*) turn segment of **2** is slightly less effective than the (*R*,*S*) segment of **1** as a hairpin inducer. The δNH pattern in Table 1 for **2** is very similar to that for **1**, suggesting that the major rotamers of both diastereomers display similar intramolecular hydrogen bonding patterns. This conclusion is reinforced by the N−H stretch IR data for **2**, which are quite similar to the corresponding data for **1**; the single broad hydrogen bonded band at 3354 cm^{-1} observed for **2** corresponds to the partially resolved bands at 3373 and 3333 cm^{-1} observed for **1**. The small non-hydrogen bonded N−H band at 3425 cm^{-1} for **2** matches a very similar feature in the spectrum of **1**.

The data for **3** and **4** are similar to one another and quite distinct from the data for **1** and **2**. For both **3** and **4**, all δNH values of the major rotamers are relatively far upfield, which suggests that intramolecular hydrogen bonding is limited in each case and that there is no single preferred internal hydrogen bonding pattern for either **3** or **4**. This conclusion is supported by the IR data for **3** and **4**, which show two major bands in the non-hydrogen bonded region, at 3455 and 3425 cm^{-1}. The band at 3455 cm^{-1} can be assigned to NH3 in the non-hydrogen bonded state on the basis of extensive precedent. Secondary amide NH groups bearing a methyl group, like NH3, display non-hydrogen bonded N−H stretch bands that are typically 20 cm^{-1} higher in energy than those of secondary amide NH groups with an adjacent alkyl branch point,[37] as is the case for NH1 and NH2. Thus, the 3425 cm^{-1} bands for **3** and **4** are assigned to non-hydrogen bonded NH1 and/or NH2. The data for **3** and **4** indicate that neither homochiral reverse turn segment is an effective promoter of hairpin formation.

The comparison among diastereomers **1**−**4** shows that β-peptide hairpin formation is very sensitive to reverse turn configuration. These findings are consistent with earlier studies, in which we found that the heterochiral dinipecotic acid segment allows 12-membered ring hydrogen bond formation (i.e., this segment can adopt a reverse turn conformation), while the homochiral dinipecotic acid segment does not allow formation of the 12-membered ring hydrogen bond.[6b]

Conformational Analysis of Tetra-β-peptides Containing β-Alanine Strand Residues. Two types of antiparallel sheet interactions are possible for β-peptide strand residues, depending on whether the strand residues favor anti or gauche $NC_\beta-C_\alpha C(=O)$ torsion angles;[6a] diastereomers **6** and **7** were examined to determine whether turn segment configuration influences the formation of a hairpin with gauche strand residues. We have previously pointed out that anti $NC_\beta-C_\alpha C(=O)$ torsion angles, as observed for the α,β-disubstituted residues in **1**−**4**, result in

(36) Solvent effects provide evidence that the multiplicity of the NMR resonances arises from amide rotamers. In CD_3OH, **1** displays three sets of NH resonances, with a ratio of 4.3:2.8:1 at 15 °C and 3.3:2.1:1 at 24 °C.

(37) Boussard, G.; Marraud, M. *J. Am. Chem. Soc.* **1985**, *107*, 1825 and references therein.

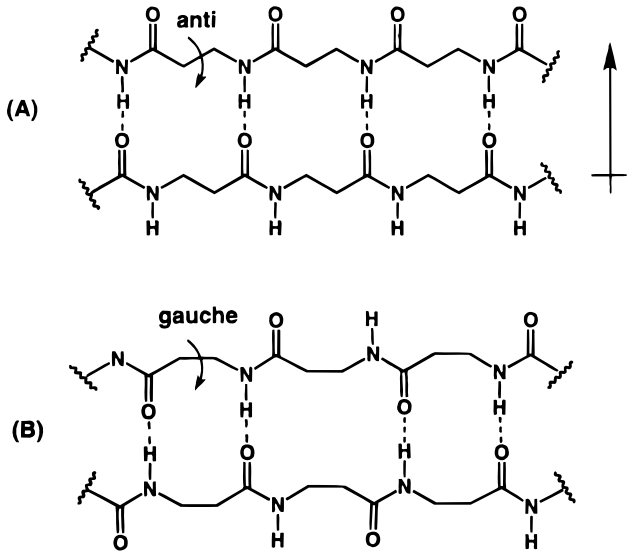

Figure 3. Two possible types of antiparallel sheet interaction between β-peptide strands: (A) polar sheet, because all carbonyls are oriented similarly; (B) nonpolar sheet, because carbonyl orientations alternate along each strand.

a sheet with a strong dipole because all of the strand carbonyls point in approximately the same direction (Figure 3).[6a] In contrast, gauche $NC_\beta-C_\alpha C(=O)$ torsion angles prevent a strong dipole from developing because the carbonyls of adjacent residues are oriented in opposite directions. β-Alanine strand residues have been shown to adopt gauche $NC_\beta-C_\alpha C(=O)$ torsion angles and form the nonpolar type of antiparallel sheet when attached to a non-β-peptide turn segment.[6a] Tetra-β-peptides **6** and **7** allow us to determine how dinipecotic acid linkers affect sheet interactions between β-alanine strands; since the strand residues are achiral in this series, only two diastereomeric forms are possible.

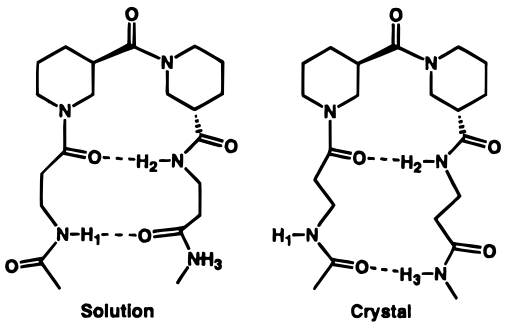

6

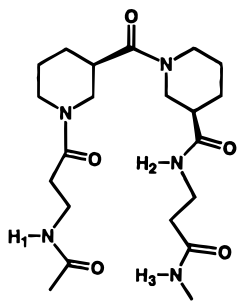

7

NMR and IR data reveal that the heterochiral dinipecotic acid turn segment (in **6**) promotes sheet interactions between

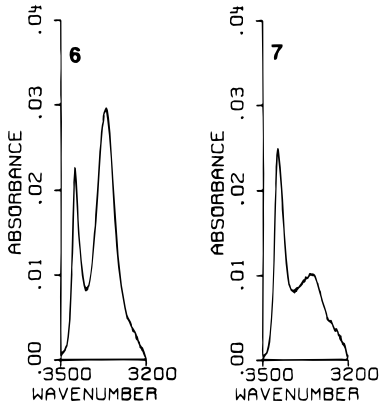

Figure 4. N−H stretch FT-IR data for 1 mM samples in CH_2Cl_2 at room temp, after subtraction of the spectrum of pure CH_2Cl_2. From left to right: **6**, maxima at 3453 and 3342 cm^{-1}; **7**, maxima at 3449 and 3338 cm^{-1}.

β-alanine strands, at least to some extent, while the homochiral turn segment (in **7**) does not promote such interactions at all. NMR data indicate the presence of at least three amide rotamers in slow exchange for **6** in CD_2Cl_2, but one of these rotamers is predominant (∼70%). For the major rotamer of **6**, δNH1 (7.49) and δNH2 (7.87) both indicate amide protons that are intramolecularly hydrogen bonded to a large extent, while δNH3 (5.84) indicates an amide proton that experiences little hydrogen bonding. These data are consistent with the interstrand hydrogen bonding pattern expected if the β-alanine residues adopt gauche $NC_\beta-C_\alpha C(=O)$ torsion angles and engage in nonpolar sheet formation (Figure 3); this proposed conformation is indicated by the "solution" structure drawn for **6**. The major rotamer conformation for **6** in CD_2Cl_2 is not as securely established as for **1**, because resonance overlap inhibits two-dimensional NMR analysis. Nevertheless, it is clear from the data that the major rotamer of **6** and the major rotamer of **1** have dramatically different internal hydrogen bonding patterns in CD_2Cl_2. The δNH values of the minor rotamers of **6** fall between 6.00 and 7.00, suggesting that there is relatively little internal hydrogen bonding in these species.

Diastereomer **7** shows evidence of at least two rotamers in CD_2Cl_2, but none is predominant. All δNH values for **7** are below 7.00, which suggests that no amide proton is internally hydrogen bonded to a large extent in either of the rotamers. N−H stretch region IR data for **6** and **7** (Figure 4) support the conclusions derived from NMR data. The large band at 3342 cm^{-1} observed for **6** indicates substantial intramolecular N−H- -O=C hydrogen bonding, while the presence of only a small band at 3338 cm^{-1} for **7** shows that this molecule experiences very little internal hydrogen bonding.

The crystal structure of **6** (Figure 5) reveals a hairpin conformation that is different from the major conformation indicated by the δNH data for **6** in methylene chloride solution. In the solid state, the β-alanine strand residues display anti $NC_\beta-C_\alpha C(=O)$ torsion angles, and the intramolecular hydrogen bonding pattern is analogous to that observed for **5** in the solid state and for **1** and **2** in solution. This result is a reminder that the conformation of a flexible molecule in the solid state may not reflect the conformational preferences of that molecule in solution.

Solid-State Structural Comparisons. The availability of crystal structures for three hairpin-forming molecules, **5**, **6**, and **8** (ref 6a), provides an opportunity for detailed structural comparisons that could help identify key features of sheet secondary structure among β-peptides. Table 2 provides backbone torsion

Table 2. Backbone Torsion Angles of β-Amino Acid Residues in Crystalline Hairpin Molecules[a,b]

	residue 1			residue 2			residue 3			residue 4		
β-peptide	ϕ	θ	ψ	ϕ	θ	ψ	ϕ	θ	ψ	ϕ	θ	ψ
5	94.4	−164.9	−122.3	115.7	−175.2	81.7	−117.4	−176.6	−71.2	130.1	173.1	−135.6
6a	176.2	174.7	−173.4	98.3	−179.5	82.3	−119.3	179.4	−59.6	−161.1	−178.4	160.5
6b	−171.5	171.4	−168.3	99.3	−175.3	81.3	−124.2	179.7	−59.3	−176.9	175.6	−172.9
8a	134.4	−178.7	−117.9	–	–	–	–	–	–	110.5	174.8	−132.7
8b	148.5	171.2	−142.9	–	–	–	–	–	–	110.5	174.8	−132.7

[a] There were two independent molecules in crystalline **6** and **8**. [b] The backbone torsion angles are defined as:

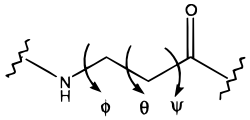

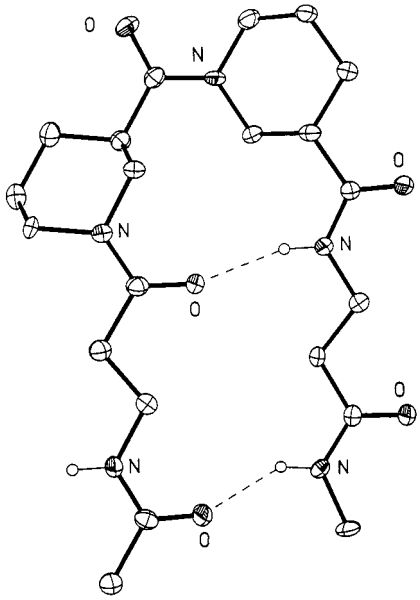

Figure 5. Ball-and-stick representation of the solid state conformation of **6**. All hydrogen atoms, except those attached to nitrogen, have been omitted. Hydrogen bonds are indicated with dotted lines. The nitrogen and oxygen atoms are labeled.

angles for each β-amino acid residue in each of the three structures. We follow conventional peptide nomenclature in using ϕ to designate the intraresidue torsion adjacent to N (i.e., (O═)-CN−$C_\beta C_\alpha$) and ψ to designate the intraresidue torsion adjacent to C═O (i.e., $C_\beta C_\alpha$−C(═O)N). We follow Seebach et al.[38] in using θ to designate the central NC_β−C_αC(═O) torsion angle in each residue. There were two independent molecules in the crystals of **6** and **8**, and both sets of torsion angle data are provided. All strand residues display anti θ torsion angles (near 180°). In contrast, there is significant variation among ϕ and ψ

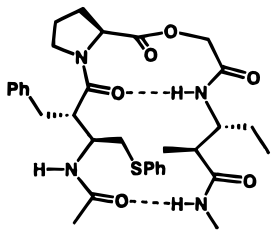

8

Table 3. Intramolecular Hydrogen Bond Parameters in Crystalline Hairpin Molecules[a]

	inner H-band		outer H-band	
β-peptide	d(H···O)[b]	∠(N-H···O)[c]	d(H···O)[b]	∠(N-H···O)[c]
5	2.15	170.8	2.20	172.3
6a	2.12	162.1	2.02	147.0
6b	2.17	161.2	2.02	150.4
8	2.09	149.7	2.20	144.7

[a] H-bond definitions:

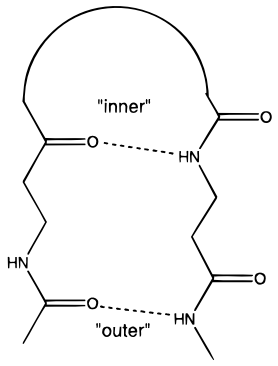

[b] O···H separation in Å. [c] N−H···O angle in degrees.

torsion angles of the strand residues. The nipecotic acid residues of **5** and **6** also display anti θ torsion angles, presumably enforced by the six-membered ring. The ϕ torsion angles of the nipecotic acid residues are not anti and vary significantly, reflecting the sp^2 hybridization of the nitrogen atom.

Table 3 provides geometric parameters for the intramolecular hydrogen bonds in the crystal structures of **5**, **6,** and **8**. The average O- -H distance and N−H- -O angle of the "inner" and "outer" hydrogen bonds in these structures are similar. The N−H- -O angles of these β-peptide sheet hydrogen bonds are comparable to the average N−H- -O angles (160°) for interstrand hydrogen bonds in protein antiparallel β-sheets.[40] The β-peptide hydrogen bonds are somewhat longer, and therefore perhaps less favorable, than those in protein β-sheets (average O- -H = 1.96 Å).[40]

Discussion

Our results show that the reverse turn conformation adopted by a heterochiral dinipecotic acid segment promotes antiparallel sheet interactions between attached strand residues, while a homochiral dinipecotic acid segment is unable to induce sheet formation. This distinction holds for both α,β-disubstituted strand residues, which prefer anti NC_β−C_αC(═O) torsion angles, and β-alanine strand residues, which prefer gauche NC_β−C_αC-

(38) Abele, S.; Seiler, P.; Seebach, D. *Helv. Chim. Acta* **1999**, *82*, 1559.
(39) Baker, E. N.; Hubbard, R. E. *Prog. Biophys. Mol. Biol.* **1984**, *44*, 97.
(40) Wüthrich, K. *NMR of Proteins and Nucleic Acids*; Wiley: New York, NY, 1986.

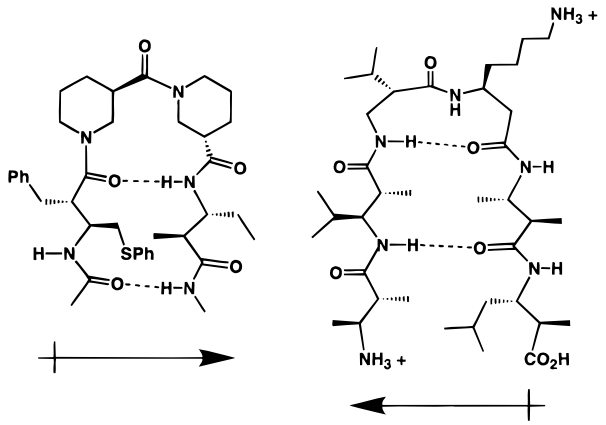

Figure 6. Comparison of β-peptide hairpin from our laboratory (left, ref 6b) and from Seebach et al. (right, ref 6c), showing how the difference in reverse turn hydrogen bonding pattern leads to a difference in the orientation of the sheet dipole.

(═O) torsion angles. We have previously shown that hairpin formation among conventional peptides (α-amino acid residues) is also strongly influenced by turn configuration: D-Pro-Xxx segments promote hairpin formation between L-residue strands, but L-Pro-Xxx segments discourage hairpin formation.[26,33] The origin of these effects differs between the two peptide classes. For conventional peptides, the critical issue is matching the local twist of the turn segment to the intrinsic twist preferred by the strand segments.[26,33] For the dinipecotic acid β-peptide reverse turns, on the other hand, the critical issue is whether the ends of the turn can come together to form the 12-membered ring hydrogen bond.

The β-peptide hairpin results presented here and in previous papers from our laboratory[6a,b] are complemented by a β-peptide hairpin study very recently reported by Seebach et al.[6c] The design strategy employed by Seebach and co-workers[6c] closely follows our earlier efforts[6a,b] in two respects. First, Seebach et al. have used the hairpin folding motif to generate soluble sheets; these workers report that individual β-peptide strand segments are insoluble,[6c] which mirrors the well-known behavior of conventional hydrophobic peptides that are prone to adopt extended β-strand conformations. Second, Seebach et al. have used strand residues with the α,β-disubstitution pattern that we previously showed to be optimal for sheet secondary structure.[6a] The Seebach hairpin differs from our hairpins, however, in the reverse turn segment (Figure 6). Our dinipecotic acid reverse turn involves a 12-membered ring hydrogen bond between C═O of residue *i* and N−H of residue *i* + 3.[6b] In contrast, the Seebach reverse turn, formed across a di-β-peptide segment composed of an α-substituted residue followed by a β-substituted residue, involves a 10-membered ring hydrogen bond between C═O of residue *i* and N−H of residue *i* − 1.[6c] As shown in Figure 6, this difference in reverse turn structure leads to a switch in the directionality of the sheet dipole relative to the N- and C-termini of the β-peptide.

Comparisons among the data now available for several different β-peptide hairpins in organic solvents reveal general trends in sheet secondary structure formed by β-amino acid residues and suggest guidelines for the design of larger sheets that will fold in aqueous solution. The regular secondary structures of conventional peptides can be identified via NOEs involving backbone atoms of residues that are not adjacent in sequence;[40] NOEs characteristic of standard antiparallel β-sheet secondary structure include C_αH- -C_αH between non-hydrogen bonded residue pairs and NH- -NH between hydrogen bonded residue pairs. Antiparallel sheets involving β-peptide residues also appear to display a characteristic pattern of backbone NOEs. In an antiparallel sheet formed by β-amino acid residues with anti $NC_\beta-C_\alpha C(=O)$ torsion angles, all of the residues in one strand are either exclusively hydrogen bond donors or exclusively hydrogen bond acceptors with regard to a neighboring strand. The three hairpins with β-peptide strands for which NOE data are available, **1** (ref 6b), **8** (ref 6a) and the hairpin of Seebach et al.,[6c] all show backbone NOEs between C_βH on the hydrogen bond acceptor strand and C_αH on the hydrogen bond donor strand (Figure 7). The different strand juxtapositions that result from the different reverse turn segments used by us[6a,b] and by Seebach et al.[6c] can be distinguished by which of the interstrand C_βH- -C_αH NOEs is observed. Our reverse turn, with a 12-membered ring hydrogen bond, leads to a C_βH- -C_αH NOE in the N-to-C direction, while the reverse turn of Seebach et al., with a 10-membered ring hydrogen bond, leads to a C_βH- -C_αH NOE in the C-to-N direction.

Side chain−side chain NOEs are often observed in β-sheets formed by conventional peptides; these NOEs help one refine the structure of the β-sheet, and they frequently indicate cross-strand interactions that stabilize the sheet interaction. For sheets formed by α,β-disubstituted β-amino acid residues, there are two different sets of side chains that could display NOEs for each interstrand residue pairing, the β-side chain on the hydrogen donor residue and the α-side chain on the hydrogen bond acceptor residue, or the α-side chain on the donor residue and the β-side chain on the acceptor residue. Comparison of NOE data for hairpins **1** (ref 6b) and **8** (ref 6a) indicates that only one or the other of these pairings leads to side chain−side

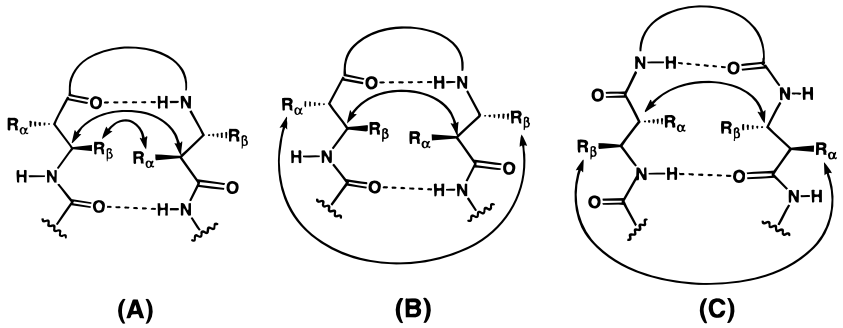

Figure 7. Summary of backbone−backbone and side chain−side chain NOEs observed for **8** (A, ref 6a), **1** (B, ref 6b) and the hairpin of Seebach et al. (C, ref 6c). In each case, there is an interstrand C_βH- -C_αH NOE, but the directionality varies C_βH on the N-terminal side/C_αH on the C-terminal side (A, B) vs C_βH on the C-terminal side/C_αH on the N-terminal side (C). In each case, NOEs are observed between one pair of side chains (designated R_α or R_β), but in A this pair is attached to the carbons bearing the hydrogens that show the backbone−backbone NOE, while in B and C this pair of side chains is attached to the "other" carbons.

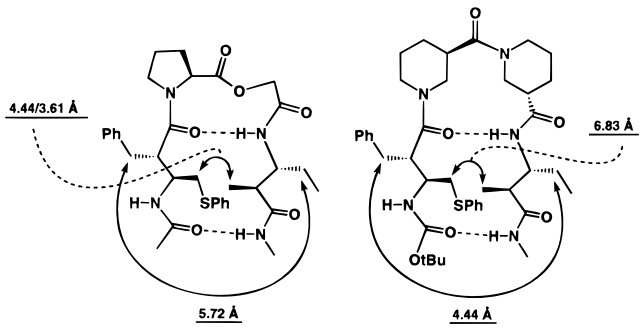

Figure 8. Nonbonded carbon−carbon distances observed in the crystal structures of **8** (left, ref 6a) and **5** (right, ref 6b). These distances are consistent with the pattern of side chain−side chain NOEs observed for **8** and **1** in solution (Figure 7A and B). Thus, the smaller separation for **8** involves the C_α substituent of the N-terminal strand and the C_β substituent of the C-terminal strand (there are two distances because of disorder in this part of the structure), corresponding to the observed side chain−side chain NOE. The smaller separation for **5** involves the C_β substituent of the N-terminal strand and the C_α substituent of the C-terminal strand, and there is a corresponding side chain−side chain NOE for **1**.

chain NOEs (Figure 7). An NOE is observed between the methylene of the β-side chain of residue 1 and the methylene of the α-side chain of residue 4 in **8** (ref 6a) while NOEs are observed between the methylene of the α-side chain of residue 1 and the methylene of the β-side chain of residue 4 of **1** (ref 6b). The crystal structures of **5** (a close analogue of **1**) and **8** reveal a variation in side chain separations that mirrors the side chain−side chain NOE differences observed between **1** and **8** in solution (Figure 8). Further inspection of the crystal structures indicates that the variation in interstrand juxtaposition between the two molecules arises at least in part from variations in the ϕ torsion angles in each strand residue (Table 2).

The side chain−side chain interaction trends noted here have important ramifications for design of β-peptide hairpins that fold in aqueous solution. Hairpin formation in water is likely to require favorable interactions between large hydrophobic side chains on neighboring strands, as is the case for conventional peptides that adopt β-hairpin conformations in aqueous solution.[41] None of the small β-peptide hairpins reported so far provides the opportunity for favorable interstrand pairing of hydrophobic side chains: the side chain pairs in these examples all have a methyl or an ethyl group on one side,[6] and these moieties are too small to provide the necessary hydrophobic driving force. We are currently using this and other design principles in an effort to generate β-peptides that display stable hairpin conformations in water.

Experimental Section

General. All melting points are uncorrected. Reagents employed were either commercially available or prepared according to a known procedure. Anhydrous CH_2Cl_2 was obtained by distillation from CaH_2. All other solvents used were reagent grade except for hexane, which was purified by distillation. Anhydrous reaction conditions were maintained under a slightly positive nitrogen atmosphere in oven-dried glassware. Silica gel chromatography was performed using 230−400 mesh silica purchased from EM Science. Routine ^{1}H NMR spectra were obtained on a Bruker AM-300 spectrometer. NMR spectra were referenced to TMS (0 ppm). Infrared spectra were obtained using a Nicolet 740 FT-infrared spectrometer. High-resolution electron impact ionization mass spectroscopy was performed using a Kratos MS-25 spectrometer.

IR Studies. High quality infrared spectra (128 scans) were obtained at 2 cm^{-1} resolution using a 1 mm CaF_2 solution cell and a Nicolet 740 FT-infrared spectrometer. All spectra were obtained in 1 mM solutions in anhydrous CH_2Cl_2 at 297 K. All compounds were dried in vacuo at elevated temperatures in the presence of P_2O_5. CH_2Cl_2 was distilled from CaH_2 and stored over activated 4 Å molecular sieves. All sample preparations were performed in a nitrogen atmosphere.

Resolution of Racemic HN-Nip-OC_2H_5 with Enantiomerically Pure Tartaric Acid. This resolution was carried out according to the published procedure.[31,32] Racemic HN-Nip-OC_2H_5 (71 mL) and D-(−)-tartaric acid (67 g) were dissolved in hot EtOH (750 mL). The solution as cooled to room temp and stored at 4 °C overnight. The resulting crystals were isolated by filtration and washed with cold EtOH. Redissolution of these crystals in hot EtOH (650 mL) followed by cooling as before gave a second batch of crystals (mp 110−130 °C). Redissolution in hot EtOH (600 mL) and cooling as before gave a third batch of crystals (mp 145−147 °C; $[\alpha]_D = -45.7$ (*c* 2, 0.2% aqueous ammonium molybdate). Redissolution in hot EtOH (600 mL) and cooling as before gave a fourth batch of crystals (mp 153−154 °C; $[\alpha]_D = -51.0$ (*c* 2, 0.2% aqueous ammonium molybdate). Redissolution in hot EtOH (650 mL) and cooling as before gave a fifth batch of crystals (mp 155−156 °C; $[\alpha]_D = -51.0$ (*c* 2, 0.2% aqueous ammonium molybdate) (lit.[32,42] mp 155−156 °C, $[\alpha]_D = -51.0$).

Resolution of Racemic Nipecotic Acid with Enantiomerically Pure Camphorsulfonic Acid. (1*R*)-(+)-10-Camphorsulfonic acid (11.62 g, 0.05 mol) was added to a stirred solution of racemic nipecotic acid (6.46 g, 0.05 mol) in acetone (100 mL). The solution was heated to reflux, and H_2O (15 mL) was added until all solids dissolved. The solution was cooled to room temperature and allowed to stir overnight. The precipitate was isolated by filtration and recrystallized three times from 6:1 acetone:H_2O to afford 1.72 g (10% yield) of the desired product as a white solid: mp 221−223 °C; $[\alpha]_D$ −25.9 (*c* 1.0, MeOH). Subsequent results indicated this salt to contain (*R*)-nipecotic acid.

Boc-(*R*)-Nip-OH. To a 0 °C solution of (*R*)-nipecotic acid (1*R*)-(+)-10-camphorsulfonic acid salt (3.62 g, 10 mmol) in MeOH (40 mL) were added Et_3N (7 mL, 50 mmol) and $(Boc)_2O$ (2.62 g, 12 mmol). After stirring 4 h at 50 °C, the solution was concentrated under reduced pressure. The residue was dissolved in water (20 mL) and acidified to pH 2−3 by adding saturated $KHSO_4$ solution. The solution was extracted with EtOAc, and the organic layer was washed with 1 N HCl and brine. The organic extract was dried over $MgSO_4$, concentrated, and dried under vacuum to afford Boc-(*R*)-Nip-OH (2.28 g, 99%) as a white solid: mp 166−167 °C (lit.[42] mp 165.8−166.6 °C); ^{1}H NMR ($CDCl_3$) δ 11.11(br s), 4.13 (br), 3.88 (dt, $J = 13.2$, 7.6 Hz), 3.01 (br), 2.87 (m), 2.48 (m), 2.06 (m), 1.69 (m), 1.46 (s); $[\alpha]_D = -52.17$ (*c* 1.15, CH_3OH) (lit.[42] $[\alpha]_D = -41.6$ (*c* 5, CH_3OH)).

HPLC Analysis of Enantiomeric Purity. Boc-Nip-OH, generated from either of the two resolution methods described, was converted to the corresponding 2-naphthylmethyl ester as follows. Boc-Nip-OH (0.25 g, 1.1 mmol) was dissolved in *N*,*N*-dimethylformamide (DMF) (5 mL), Cs_2CO_3 (0.36 g, 1.1 mmol) and 2-(bromomethyl)naphthalene (0.28 g, 1.2 mmol) were added, and the solution was stirred at room temp for 24 h. The solution was then concentrated, and the residue was dissolved in H_2O. The aqueous solution was extracted with CH_2Cl_2. The organic layer was dried over $MgSO_4$ and concentrated to give an oil. The crude product was purified by silica chromatography eluting with 1:2 ethyl acetate:hexanes to afford 0.34 g (84% yield) of the desired product as a white solid: mp 70−71 °C; ^{1}H NMR ($CDCl_3$, 300 MHz) δ 7.9−7.8 (m), 7.55−7.45 (m), 5.3 (s), 4.40−4.05 (br s), 4.00−3.85 (br d), 3.10−2.90 (br s), 2.85−2.75 (dt), 2.60−2.45 (m), 2.15−2.05 (m), 1.75−1.55 (m), 1.55−1.40 (s); FAB-MS *m*/*z* (M + Na^+) calcd for $C_{22}H_{27}NO_4Na$ 392.0, obsd 392.6.

Chiral HPLC was performed on the 2-naphthylmethyl ester of Boc-Nip using a 250 × 4.6 mm Chiracel OD column (Chiral Technologies Inc., Exton, PA) eluting with 9:1 hexanes:2-propanol at a flow rate of 1.0 mL/min. The retention times for the (*R*)- and (*S*)-isomers were 8.8

(41) (a) de Alba, E.; Rico, M.; Jiménez, M. A. *Protein Sci.* **1997**, *6*, 2548. (b) Maynard, A. J.; Sharman, G. J.; Searle, M. S. *J. Am. Chem. Soc.* **1998**, *120*, 1996.

(42) Zheng, X.; Day, C.; Gollamudi, R. *Chirality* **1995**, *7*, 90.

and 9.4 min. After each type of resolution, optical purity of each enantiomer ≥99% (i.e., ≥98% e.e.).

Boc-(*R*)-Nip-(*S*)-Nip-OCH$_3$. (*S*)-Nip-OCH$_3$ was prepared from *S*-nipecotic acid (1*R*)-(+)-10-camphorsulfonic acid salt with $SOCl_2$ in MeOH. Boc-(*R*)-Nip-OH (1.72 g, 7.5 mmol), (*S*)-Nip-OCH$_3$ (7.5 mmol), and HOBt (1.22 g, 9 mmol) were dissolved in DMF (100 mL). The solution was cooled to −15 °C, and Et_3N (3.13 mL, 22.5 mmol) and EDC (1.73 g, 9 mmol) were added. After stirring for 40 h at room temp, the solution was concentrated under reduced pressure. The residue was dissolved in EtOAc and washed with 1 N HCl, saturated $NaHCO_3$, and brine. The organic extract was dried over $MgSO_4$ and concentrated. The crude product was purified by silica chromatography (hexanes: EtOAc = 1:1), yielding Boc-(*R*)-Nip-(*S*)-Nip-OCH$_3$ (2.58 g, 97%) as a white solid: mp (recrystallized from 1:5 EtOAc:hexane) 86.5−88 °C. ^{1}H NMR (CD_2Cl_2) δ 4.50 (br d), 4.02 (br d), 3.78 (br t), 3.66 (s), 3.42 (m), 3.09−2.94 (m), 2.81 (m), 2.66 (m), 2.56−2.52 (m), 2.05 (m), 1.81 (m), 1.65 (m), 1.44 (s); $[\alpha]_D$ = +23.0 (*c* 1.20, $CHCl_3$); EI-MS *m*/*z* (M^+) calcd for $C_{18}H_{30}O_5N_2$ 354.2155, obsd 354.2151.

Boc-(*R*)-Nip-(*S*)-Nip-OH. To a 0 °C solution of Boc-(*R*)-Nip-(*S*)-Nip-OCH$_3$ (1.55 g, 4.37 mmol) in THF (20 mL) was added dropwise a solution of LiOH·H_2O (0.19 g, 4.6 mmol) in H_2O (10 mL). After 4 h at room temp, the solution was concentrated, diluted with H_2O, and extracted with Et_2O. The aqueous layer was acidified to pH 2−3 with 1 N HCl. The solution was extracted with EtOAc, and the organic layer was dried over $MgSO_4$, concentrated, and dried under vacuum to afford Boc-(*R*)-Nip-(*S*)-Nip-OH (1.45 g, 97%) as a white solid: mp (recrystallized from 1:10 EtOAc:hexane) 166−167 °C; ^{1}H NMR (CD_2Cl_2) δ 9.55 (br), 4.44 (br d), 4.05 (br d), 3.83 (m), 3.40 (m), 3.14 (br t), 2.93 (m), 2.84−2.56 (m), 2.45 (m), 2.10 (m), 1.83 (m), 1.66 (m), 1.43 (s); $[\alpha]_D$ = +17.4 (*c* 1.08, $CHCl_3$); EI-MS *m*/*z* (M^+) calcd For $C_{17}H_{28}O_5N_2$ 340.1998, obsd 340.1998.

Boc-(*R*)-Nip-(*S*)-Nip-β-Ala-NHCH$_3$. Boc-(*R*)-Nip-(*S*)-Nip-OH (0.50 g, 1.46 mmol), β-alanine *N*-methylamide hydrochloride (0.27 g, 2.0 mmol) and HOBt (0.27 g, 2.05 mmol) were dissolved in DMF (25 mL). The solution was cooled to −15 °C, and Et_3N (0.6 mL, 3.60 mmol) and EDC (0.39 g, 2.05 mmol) were added. After stirring for 36 h at room temperature, the solution was concentrated under reduced pressure. The residue was dissolved in CH_2Cl_2 and washed with 1 N HCl, saturated $NaHCO_3$ and brine. The organic extract was dried over Na_2SO_4 and concentrated. The crude product was purified by silica chromatography (EtOAc:MeOH = 30:4), yielding Boc-(*R*)-Nip-(*S*)-Nip-β-Ala-NHCH$_3$ (0.57 g, 94%) as a white solid: mp (recrystallized from 1:1 EtOAc:hexane) 203−205 °C; ^{1}H NMR ($CDCl_3$) δ 7.43 (br, with minor rotamer at 6.67), 6.39 (br, with minor rotamer at 6.09), 4.56 (m), 4.22−3.99 (m), 3.69 (m), 3.66−3.43 (m), 3.30 (m), 3.08 (m), 2.79 (t), 2.68 (m), 2.47 (m), 2.35 (t), 2.28 (m), 1.95−1.68 (m), 1.47 (s); FAB-MS *m*/*z* (M^+ + Na) calcd for $C_{21}H_{36}N_4O_5Na$ 447.5, obsd 447.7.

Boc-β-Ala-(*R*)-Nip-(*S*)-Nip-β-Ala-NHCH$_3$. Boc-(*R*)-Nip-(*S*)-Nip-β-Ala-NHCH$_3$ (0.28 g, 0.66 mmol) was dissolved in 4 N HCl in dioxane (2.5 mL). After 2 h, the solvent was removed by a stream of N_2, and the residue was dried under vacuum. The resulting solid (HN−(*R*)-Nip-(*S*)-Nip-β-Ala-NHCH$_3$·HCl), Boc-β-alanine (0.19 g, 0.98 mmol) and HOBt (0.12 g, 0.92 mmol) were dissolved in DMF (10 mL). The solution was cooled to −15 °C, and NMM (0.18 mL, 1.58 mmol) and EDC (0.17 g, 0.92 mmol) were added. After stirring for 36 h at room temperature, the solution was concentrated under reduced pressure. The residue was dissolved in CH_2Cl_2 and washed with 1 N HCl, saturated $NaHCO_3$ and brine. The organic layer was dried over Na_2SO_4 and concentrated. The crude product was purified by silica chromatography (EtOAc:MeOH = 6:1), yielding Boc-β-Ala-(*R*)-Nip-(*S*)-Nip-β-Ala-NHCH$_3$ (0.31 g, 96%) as an oil. ^{1}H NMR ($CDCl_3$) δ 7.78 (br s), 6.15 (br s), 6.09 (br s), 4.62 (m), 4.11 (m), 3.8 (m), 3.69−3.49 (m), 3.38 (m), 3.03 (m), 2.77 (d, *J* = 4.5 Hz), 2.61−2.43 (m), 1.89−1.72 (m), 1.42 (s); EI-MS *m*/*z* (M^+) calcd for $C_{24}H_{41}O_6N_5$ 495.3057, obsd 495.3049.

Ac-β-Ala-(*R*)-Nip-(*S*)-Nip-β-Ala-NHCH$_3$ (6). Boc-β-Ala-(*R*)-Nip-(*S*)-Nip-β-Ala-NHCH$_3$ (0.20 g, 0.40 mmol) was dissolved in 4 N HCl in dioxane (2 mL). After 2 h, the solvent was removed under a stream of N_2, and the residue was dried under vacuum. This residue (H_2N-β-Ala-(*R*)-Nip-(*S*)-Nip-β-Ala-NHCH$_3$·HCl) was dissolved in CH_2Cl_2 (5 mL) and cooled to 0 °C. To this solution were added Et_3N (0.11 mL, 0.80 mmol) and acetic anhydride (47 mL, 0.46 mmol). After stirring for 15 h at room temperature, the solution was concentrated under reduced pressure. The residue was purified by silica chromatography (EtOAc:MeOH = 2:1), yielding 6 (0.12 g, 68%) as a white solid: mp (recrystallized from 10:1:70 EtOAc:MeOH:hexane) 155−157 °C; ^{1}H NMR (CD_2Cl_2, 500 MHz) δ 7.87 (br s), 7.49 (br s), 5.84 (br s), 4.64 (d, *J* = 13.0 Hz), 4.54 (d, *J* = 11.5 Hz), 4.14 (d, *J* = 13.0 Hz), 3.83 (d, *J* = 16.0 Hz), 3.61−3.38 (m), 3.29 (m), 3.04 (td, *d* = 12.1, 6.0 Hz), 2.97 (t, *J* = 12.7 Hz), 2.74 (d, *J* = 5.0 Hz), 2.64−2.57 (m), 2.55 (m), 2.49 (m), 2.45 (m), 2.37 (m), 1.95−1.72 (m), 1.54 (s), 1.48−1.26 (m); EI-MS *m*/*z* (M^+) calcd for $C_{21}H_{35}O_5N_5$ 437.2638, obsd 437.2644; IR (CH_2Cl_2) 3453, 3342, 1662, 1633, 1530 cm^{-1}. Crystals of **7** suitable for X-ray analysis were grown from a solution of CH_2Cl_2−MeOH−hexane.

Ac-β-Ala-(*R*)-Nip-(*R*)-Nip-ββ-Ala-NHCH$_3$ (7). The compound was synthesized by a route similar to that used for **6**. ^{1}H NMR (CD_2Cl_2) δ 6.58 (br d), 6.42 (br d), 6.18 (br d), 4.43 (br t), 4.09 (br d), 3.67 (m), 3.46 (m), 3.21 (m), 3.04 (m), 2.85 (m), 2.74 (d, *J* = 4.2 Hz), 2.58 (m), 2.48 (m), 2.35 (m), 1.89 (s), 1.86−1.44 (m); EI-MS *m*/*z* (M^+) calcd for $C_{21}H_{35}O_5N_5$ 437.2638, obsd 437.2627; IR (CH_2Cl_2) 3338, 1668, 1634, 1515 cm^{-1}.

Tetra-β-peptides **1**−**4** were prepared by routes similar to that described above for **6** (β-amino acids were coupled by using EDC and HOBt in DMF). Synthesis of the terminal β-amino acid residues common to **1**−**4** has been previously described in detail (ref 30 and Supporting Information for ref 6a).

Tetra-β-peptide 1: mp (recrystallized from 1:7 $CHCl_3$:heptane) 214.5−217 °C; ^{1}H NMR (CD_2Cl_2, 500 MHz) δ 7.70 (d, *J* = 9.5 Hz), 7.49(d, *J* = 4.8 Hz), 7.38−7.15 (m), 5.80 (d, *J* = 10.5 Hz), 4.86 (m), 4.64 (d, *J* = 13.0 Hz), 4.57 (d, *J* = 12.5 Hz), 4.29 (d, *J* = 12.5 Hz), 4.05 (m), 3.52 (d, *J* = 11.5 Hz), 3.29 (dd, *J* = 17.5, 8.0 Hz), 3.17 (d, *J* = 14.0 Hz), 3.09 (t, *J* = 17.5, 12.5 Hz), 2.96 (dd, *J* = 19.5, 7.8 Hz), 2.90 (d, *J* = 8.0 Hz), 2.74 (d, *J* = 7.8 Hz), 2.72 (m), 2.54 (m), 2.40 (td, *d* = 13.0, 4.3 Hz), 2.28 (t, *J* = 12.0 Hz), 2.19 (t, *J* = 11.5 Hz), 1.99 (m), 1.92 (s), 1.89 m), 1.76 (d, *J* = 13.5 Hz), 1.70−1.60 (m), 1.53−1.26 (m), 1.15 (m), 1.14 (d, *J* = 6.1 Hz), 0.93 (t, *J* = 7.3 Hz), −0.52 (m); FAB-MS *m*/*z* (M^+ + Na) calcd for $C_{38}H_{53}N_5O_5SNa$ 714.9, obsd 714.3; IR (CH_2Cl_2) 3421, 3373, 3333, 1668, 1635, 1615, 1538 cm^{-1}.

Tetra-β-peptide 2: mp 136−140.5 °C; ^{1}H NMR (CD_2Cl_2, 500 MHz) δ 7.41 (d, *J* = 8.5 Hz, with minor rotamer at 7.21), 7.36−7.10 (m), 6.80 (d, *J* = 9.8 Hz, with minor rotamer at 7.32), 5.81 (d, *J* = 10.0 Hz, with minor rotamer at 6.20), 4.85 (m), 4.63 (d, *J* = 13.0 Hz), 4.55 (d, *J* = 13.5 Hz), 4.12 (m), 3.68 (d, *J* = 10.5 Hz), 3.41 (m), 3.25 (m), 3.04 (m), 2.97−2.87 (m), 2.76 (d), 2.73 (m), 2.48−2.27 (m), 2.12 (t, *J* = 12.3 Hz), 1.94 (m), 1.85−1.62 (m), 1.55 (s), 1.40 (m), 1.26 (m), 1.05 (d), 0.95 (t, *J* = 8.3 Hz), 0.87 (m); FAB-MS *m*/*z* (M^+ + Na) calcd for $C_{38}H_{53}N_5O_5SNa$ 714.9, obsd 714.0; IR (CH_2Cl_2) 3425, 3357, 3355, 1668, 1635, 1615, 1533 cm^{-1}.

Tetra-β-peptide 3: mp 132−136 °C; ^{1}H NMR (CD_2Cl_2, 500 MHz) δ 7.34−7.12 (m), 5.90 (d, *J* = 9.0 Hz, with minor rotamers at 6.86 and 5.70), 6.14 (br, with minor rotamers at 6.49 and 6.43), 6.15 (br, with minor rotamers at 6.42 and 5.84), 4.56 (m), 4.27 (m), 4.21 (d, *J* = 12.0 Hz), 3.95 (m), 3.85 (m), 3.47−3.34 (m), 3.29−3.14 (m), 2.96−2.73 (m), 2.67 (s), 2.61 (br d), 2.37−2.14 (m), 2.12−2.06 (m), 2.04 (m), 1.86 (s), 1.81−1.58 (m), 1.53 (s), 1.50 (m), 1.40 (m), 1.29 (m), 1.27−1.09 (m), 1.07 (d, *J* = 13.5 Hz), 0.95−0.85 (m); FAB-MS *m*/*z* (M^+ + Na) calcd for $C_{38}H_{53}N_5O_5SNa$ 714.9, obsd 714.0; IR (CH_2Cl_2) 3454, 3425, 3378, 3337, 1672, 1629, 1510 cm^{-1}.

Tetra-β-peptide 4: mp 138−142 °C; ^{1}H NMR (CD_2Cl_2, 500 MHz) δ 7.31−7.10 (m), 6.45 (br t, with minor rotamers at 6.22 and 6.12), 5.73 (br, with minor rotamers at 6.08 and 5.69), 5.88 (br, with minor rotamer at 6.42), 4.52 (d, *J* = 13.0 Hz),), 4.31 (m), 3.95−3.84 (m), 3.59−3.43 (m), 3.37−3.01 (m), 2.98−2.87 (m), 2.78 (m), 2.74 (d, *J* = 7.2 Hz), 2.4 (m), 2.32 (m), 2.19 (m), 1.98 (m), 1.86 (d, *J* = 6.5 Hz), 1.71 (m), 1.58−1.43 (m), 1.32 (m), 1.10 (d, *J* = 7.0 Hz), 0.96 (m), 0.89 (m); FAB-MS *m*/*z* (M^+ + Na) calcd for $C_{38}H_{53}N_5O_5SNa$ 714.9, obsd 714.3; IR (CH_2Cl_2) 3455, 3425, 3338, 1676, 1629, 1549, 1510 cm^{-1}.

Crystallography of 6: $C_{21}H_{35}N_5O_5$, fw = 437.54, colorless prism, 0.24 × 0.10 × 0.06 mm, crystal system: triclinic, space group: *P*1, *a* = 9.1329(9) Å, *b* = 10.0437(10) Å, *c* = 13.6403(13) Å, α = 75.350(2)°, *β* = 71.602(2)°, *γ* = 71.618(2)°, *V* = 1110.20(19) Å^3, *Z* = 2, *T* = 133(2) K, R = 0.0558, wR(all data) = 0.1184, GOF = 0.944, Bruker SMART/P4 diffractometer, *λ* = 0.71073 Å. The data were corrected for absorption (T_{min} = 0.798, T_{max} = 0.976). The structure was solved by direct methods and refined by full-matrix least squares on F^2 (ref 43). The non-hydrogen atoms were refined with anisotropic displacement parameters. Hydrogen atoms were originally positioned by geometry and were refined isotropically using a riding model.

(43) Sheldrick, G. M. *SHELXTL*, version 5, Reference Manual; Siemens Analytical X-ray Instruments: 6300 Enterprise Dr., Madison, WI, 1994; pp 53719−1173.

Acknowledgment. This research was supported by the National Institutes of Health (GM56415). Y.J.C. was supported in part by a fellowship from the Korea Science and Engineering Foundation, H.E.S. by a National Research Service Award (T32 GM08923), and S.K. by a fellowship from the Fonds der Chemischen Industrie. NMR equipment was purchased in part with funds from the NIH (S1O RRO 4981), and crystallographic equipment in part with funds from the NSF (CHE-9310428).

Supporting Information Available: Crystallographic data for **6** (PDF). This material is available free of charge via the Internet at http://pubs.acs.org.

JA993416P